19th ICAS-Congress/AIAA Aircraft Systems Conference
Anaheim, CA, USA 18 - 23 September 1994

Unsteady Surface Pressure Characteristics on Helicopter Blades: A Key to the Physics of Rotor Noise

Hanno Heller, Klaus-J. Schultz, Syed R. Ahmed, Wolf Splettstoesser

DLR Institute of Design Aerodynamics
- Technical Acoustics -
DLR Braunschweig Research Center, Germany

Abstract

There are a number of approaches to predict helicopter rotor noise. The most common of these is the „Acoustic Analogy Approach" where (aerodynamic) source characteristics at and near the rotor blade are used as input into appropriate acoustic codes. Aerodynamic source characteristics may be determined by means of certain computational schemes, such as linearized potential flow methods (lifting line, lifting surface, unsteady panel methods) and full potential or Euler methods to yield the unsteady pressures on the blade surface or the perturbation velocity near the blade. Acoustic codes, such as the - meanwhile „classical" - 'Ffowcs Williams and Hawkings formulation' may then be employed to compute the radiated acoustics. The key to validating the various aerodynamic and acoustic codes is the availability of - experimentally determined - high quality aerodynamic and acoustic data. An appropriate benchmark experimental program (within the framework of the European Community initiated HELINOISE project) has recently been conducted to provide the needed information. This paper discusses the usage of the now available data (unsteady rotor-blade surface pressures and simultaneously measured acoustic signatures) in evaluating and improving selected prediction schemes and in furthering the understanding of the physics of rotor noise.

Nomenclature

α	shaft tilt angle
α_{TPP}	tip-path plane angle
δ	flight angle
ρ	air density
μ	advance ratio
θ	blade pitch angle
ψ	rotor azimuthal angle
Ω	rotor rotational speed
a	speed of sound
c	chord
Cp	pressure coefficient
C_T	thrust coefficient
M_{adv}	advancing blade tip Mach number
p'	sound pressure
P	blade surface pressure
r_d	distance source - observer
r	rotor coordinate
R	rotor radius
T	thrust
T_{rr}	Lighthill Tensor component in observer direction
V	flight (tunnel flow) speed
V_n	normal velocity component at source point
x	blade chordwise coordinate
x	coordinates of observer position
y	coordinates of source position

Introduction

Several computational methods to predict helicopter rotor noise have been developed in the past. Successful approaches to that extent are known under the terms ***Lighthill's acoustic analogy***, ***Kirchhoff-fomulations*** and ***computational aeroacoustics*** (use of aerodynamic methods for direct noise calculations). The most common one is the acoustic analogy approach, which util-

izes aerodynamic source inputs into appropriate acoustic codes. Of the latter, the Ffowcs Williams and Hawkings ("FWH") formulation[1] (based on the classical Lighthill formulation on aerodynamic noise) relates the radiated acoustic pressure to three aerodynamic source terms which in turn can be computed from blade geometric and rotor operational information. In order to utilize the FWH-approach, however, the details of the unsteady aerodynamic blade loading or - better still - of the blade surface pressures and of the near-blade perturbation velocities are required (in addition to blade geometrical information) to determine directly, or by appropriate approximations, these three source terms, namely the „thickness noise"-related *aerodynamic monopole term*, the „blade-loading" related *aerodynamic dipole term* and the „perturbation velocity"-related *aerodynamic quadrupole term*, which becomes important at high transonic blade tip speeds. These then combine to yield the entire noise signature (say in terms of an acoustic pressure time history at the observer position).

The aerodynamic monopole term may be determined in a fairly straightforward manner, as it is completely determined by the blade's geometry and kinematics, e.g. the rotor operational conditions; the other two terms are related to the unsteady blade surface pressures, either directly (the aerodynamic dipole) or indirectly (the aerodynamic quadrupole). In the absence of information on flow perturbation velocities near the blade (which are very hard to come by) the unsteady blade pressure is therefore the crucial physical quantity in the attempt to compute rotor noise.

Such blade pressures can now be either computed (employing aerodynamic source codes) or measured. The latter method, namely the measurement of blade pressures, is of course not the finally desired way to go in predicting rotor noise from basic principles, since, obviously, a blade would have to exist beforehand (at which point one might as well measure the sound directly rather than determine blade pressures and go the FWH-route). In the process of developing, validating and improving the aerodynamic prediction capabilities, however, such pressure data is quite indispensable. And that is where the need for high quality experimental data comes in.

Recognizing the overwhelming need for accurate aerodynamic and acoustic rotor data, the European Community (now European Union) initiated a major and comprehensive rotor research project (in the framework of the then BRITE/EURAM-Research Initiative on Aerodynamic Research) under the acronym HELINOISE, where eight European partners from research establishments, universities, small enterprises and industry joined their intellectual and financial resources to improve the understanding of the physics of helicopter rotor noise and to further the rotor noise prediction capabilities through the conduct of a benchmark experiment. Here a scaled model of the BO 105 helicopter rotor was equipped with a large number of flush mounted miniature absolute pressure sensors. The model rotor was tested in the open jet test section of the German Dutch Wind Tunnel (DNW); both the unsteady blade pressures and the ensuing acoustic radiation were measured simultaneously over an extended test matrix covering - and even exceeding - the entire operational flight envelope of the datum helicopter (encompassing hover, low speed and high speed level flight as well as descent and climb). Details of the effort are discussed in [2,3,4].

The data is presently used by the HELINOISE-Partners to validate their various aerodynamic codes for the prediction of blade pressures (as the a priori input for the FWH-formulation) and of the acoustic code as such, especially in its capability to cover transonic flow at the blade tip, where the quadrupole term becomes increasingly important.

In the subsequent sections of this paper the general theoretical **relationship between unsteady blade pressures and radiated noise** will be discussed, to lead into a short treatment of the **theoretical determination of unsteady blade surface pressures** by means of several methods, such as lifting surface methods, panel methods and Euler methods; here the importance of using a free wake or a prescribed wake will be briefly touched. This will be followed by a description of an **experimental determination of unsteady blade surface pressures** and the ensuing acoustic radiation along the HELINOISE-project; here exemplary data presented will (mostly) cover a moderate speed descent condition where blade-vortex interaction impulsive noise occurs. Next the value of the experimental (mostly HELINOISE-project related) data for **aerodynamic code validation** will be illustrated on the example of a newly developed 3-dimensional panel method to indicate the agreement between calculated and measured blade pressures for a moderate speed descent condition. The final section is devoted to illustrating the **prediction capabilities of the acoustic analogy approach** when (a) either experimentally determined blade pressures or (b) calculated blade-loadings are used as input, or if (c) both calculated blade pressures and the perturbation velocity field solution near the blade from an Euler-calculation is inserted into the dipole and the quadrupole terms.

2. Relationship of Unsteady Blade Surface Pressures and Radiated Noise

The relationship between the unsteady surface pressure on a rotating blade and the radiated noise is theoretically described by the Ffowcs William-Hawkings-equation[1], here in the form known as „Farassat Type 1".[5]

$$4\pi p'(x,t) = \frac{\partial}{\partial t}\int_S \left[\frac{\rho_o V_n}{r|1-M_r|}\right]_{ret.} dS(y)$$

$$+ \frac{1}{a_o}\frac{\partial}{\partial t}\int_S \left[\frac{P_r}{r|1-M_r|}\right]_{ret.} dS(y)$$

$$+ \frac{1}{a_o^2}\frac{\partial^2}{\partial t^2}\int_V \left[\frac{T_{rr}}{r|1-M_r|}\right]_{ret.} dV(y)$$

As previously discussed, the radiated noise depends on three source integral terms, acoustically classified after Lighthill's acoustic analogy as monopole, dipole and quadrupole. With regard to the physical meaning the monopole is called thickness term and the dipole is called loading term - both of which are surface integrals. The quadrupole term is much more complex, since this volume integral includes the complete perturbation flow field around the blade.

One of the most important parameters is the source Mach number component in the observer direction M_r. This parameter is most effective in the transonic blade tip region and for the in-plane forward radiation direction. In this case the Doppler-amplification factor $1/(1-M_r)$ assumes maximum values. Moreover, this parameter is important for all three source terms, as to be seen in the FWH-equation above.

The first source term, the **thickness term** - in addition - depends only on the blade geometry and the flight condition. The normal component of the surface velocity V_n is proportional to the free stream velocity multiplied by the local blade surface slope. Thus the *blade thickness* is here the governing parameter. Thickness noise is radiated predominantly in the in-plane forward direction.

The direct connection between blade pressures and radiated noise is described by the second source term - the **loading term**. Here $P_r \bullet dS$ is the blade pressure force component in observer direction on the source panel. The radiated loading noise is proportional to the time derivative of this parameter multiplied by the Doppler amplification factor at the retarded time (emission time). Because the main component of the loading acts normal to the blade the component in observer direction is most effective in this direction. But in combination with the Doppler amplification factor - which is most effective in the in-plane radiation direction - the loading noise is directed more or less oblique to the rotor plane. It should be understood that loading noise occurs already at constant loading during the rotation as in the hover case. This „basic" loading noise is caused by the time derivative of the Doppler amplification factor only. If the blade pressure is highly unsteady (as would be the case for blade vortex interaction conditions) the loading noise increases rapidly if the impulsive blade pressure content is located in an azimuthal range where the Doppler amplification factor becomes a maximum.

The third source term, the **quadrupole term,** is a complex volume integral including the Lighthill-tensor component T_{rr} in observer direction. The most important part of this term is the blade-parallel perturbation velocity square in observer direction. Assuming the perturbation velocity square to be most efficient near the rotating blade and integrating this quadrupole parameter normal to the blade the quadrupole volume integral is reduced to a surface integral, following the „momentum thickness approach" of Yu, Caradonna and Schmitz [6]. If the perturbation velocity field, for example, was provided by a computational fluid dynamics (CFD) code, then the acoustic calculation is substantially simplified.

On the other hand, the perturbation velocity square (i.e. the quadrupole parameter) on the blade surface is related to the blade pressure via the Bernoulli-equation. In case a plausible relationship between the quadrupole parameter integral normal to the blade and the parameter on the surface can be found, the quadrupole noise can be approximately calculated also on the basis of the blade pressure information. Like the thickness term the quadrupole term is most effective in the in-plane forward direction because it is the perturbation velocity component parallel to the rotor plane which is dominant. The quadrupole part is important at high tip speeds when the advancing tip Mach numbers, M_{adv}, approaches (and exceeds) a value of 0.9.

In general then, the acoustic calculation can be split into two different problems when considering helicopter rotor impulsive noise (constituting the most objectionable and intrusive kind of helicopter rotor noise):

- for low-speed descent BVI flight conditions where the loading term would dominate, only the linear terms (monopole and dipole) of the FWH-equation are needed,
- for high-speed forward flight conditions where compressibility effects become important, the nonlinear quadrupole term of the FWH-equation must be included.

3. Theoretical Determination of Unsteady Blade Surface Pressures

3.1 Nature of Flow around a Helicopter Rotor

The flowfield around a helicopter rotor is extremely complex because of the concurrent occurrence of several

aerodynamic phenomena. These are three-dimensionality, unsteadiness, transonic flow regions and viscous effects.

In forward flight, unsteadiness is introduced in the flow by the cyclic variation of the free stream velocities relative to the (rotating and advancing/retreating) blades and the cyclic modulation of blade pitch, flapping and lead/lag motions. Another source of unsteadiness is due to each of the blades traversing a temporally varying flow region generated by its own wake and the wakes of preceding blades. In contrast to fixed wing aerodynamics, this mutual interference between rotor blades and their wakes is an important feature of all helicopter operational modes, but becomes dominant in hover and descent flight.

On the advancing blade, the flow can become transonic, especially in high speed forward flight, near the blade tip. The increased pitch on the retreating blade may generate pockets of dynamic stall near the blade tip and flow reversal/flow separation at the blade root. For a realistic simulation of rotor flows these unsteady viscous effects have to be modelled. As a consequence of such complicated aerodynamic phenomena, the computation of the flow around a multiblade helicopter rotor poses an enormous challenge for computational fluid dynamics (CFD).

3.2 Inviscid Flow Approaches to Compute Rotor Flow

Inviscid aerodynamics is the primary field for most of the advanced methods currently in use for rotors. As noted above, the rotor wake is a major phenomenon in almost all helicopter problems. The helical geometry of the rotor wake implies that its detailed spatial and temporal configuration is important.

The classical method to compute the flow around a rotor blade is based on the **lifting line theory**. Because of its simplicity and the modest computational effort needed, it is widely used in rotor aerodynamics. The lifting line theory follows the concept that the creation of lift by the blade is due to a single ('bound') vortex filament lying at blade quarter chord and running along the blade span. At the blade root and tip, the pressure equalization process generates the so-called root and tip vortices which may be considered as the downstream continuation of the bound vortex. These 'wake' vortices are - at the time of their emission from the blade root and tip - orientated parallel to the incident flow. Due to blade rotation and forward motion, they subsequently follow a complicated spatially distorted helical path and constitute the 'wake'.

Since the geometry of this vortex wake is difficult to determine experimentally or by theoretical means - and in conformity with the simple concept of the lifting line method - it is generally prescribed and assumed to be time invariant (see e.g. [7]). The output of a lifting line code calculation is the lift distribution over the blade span only. Blade planform, tip shape, profile etc. cannot be considered. With the help of additional information, such as measured or computed aerodynamic characteristics of the blade sections, blade planform etc., the effect of these parameters can be indirectly and aproximately considered. However a considerable amount of uncertainty is introduced in this way into the computation. Basically this information allows the computation of only the 'loading' noise.

A more sophisticated approach to evaluate the blade aerodynamics is the **lifting surface concept**. Especially when the lift variation over chord is an important design consideration (blade pitching moment and vibration susceptibility), it is necessary to replace the model of a single lifting line by that of a distribution of lifting lines over the blade chord. This concept neglects the blade thickness as the distribution is spread over a blade planform of zero thickness. Since the lifting surface model of the blade permits simulation of non-rectangular blade planforms with twist and blade tip modifications, the generated pressure difference data can be used as input for acoustic signature prediction of such configurations.

A step further is provided by the **Panel method** which permits the modeling of the aerodynamics of arbitrarily shaped bodies. Basically all geometric parameters of a real blade (profile geometry, planform, twist, tip shape etc.) can be considered in this approach. In contrast to the lifting surface theory, the Panel method calculation gives the pressure and velocity distribution on the upper and lower blade surface. A more realistic simulation of blade geometry and a corresponding detailed aerodynamic information is available as input to the acoustic codes.

As is the case with the lifting line method, the modeling of the wake in the lifting surface and panel methods can also be done either by prescribing its geometry a priori or calculating it step by step during the computation. In this latter approach, called the free wake analysis, advance knowledge of wake geometry is not needed, as this is a partial result of the time stepping solution. The quality of pressure and velocity data generated by the above explained methods depends critically on the physically realistic simulation of the rotor wake as has been indicated above. Even though a free wake analysis implies an increase in computational expense it comes closer to reality than a prescribed wake geometry which - strictly speaking - is valid for only the rotor geometry and running conditions for which it had been determined and is not transferable to other situations.

A common feature of the lifting line, lifting surface and panel methods (the so called *potential flow methods*) is the conservation of the shed vorticity in the wake. This implies that the vortical structures formed in the wake

do not dissipate in their strength - they only deform. In the real flow, however, the wake vorticity dissipates. This 'over simulation' of the wake vorticity in the potential flow methods has influence on the pressure prediction and consequently on the predicted acoustics.

The main drawback of these *linearised potential flow methods* is their inability to capture compressibility effects such as the formation of transonic flow regions and shocks near the blade tip during high speed forward flight. Treatment of such non-linear effects is the domain of 'field methods' such as the **full potential** or **Euler methods**. Also here due to considerations of computational expense and dependability of the predictions the right strategy has to be chosen to capture the wake.

Typical of the present situation, two approaches are frequently used to capture the wake. In the first (see for example [8])a full potential method simulates the rotor blade aerodynamics and the wake is modeled in an Eulerian-Lagrangian fashion by "markers" which convect with the flow and carry the shed vorticity information. In this way the compressible flow around the blade and a non-dissipative convection of the wake is calculated. However, the main disadvantage of this approach is the need to know the wake topology a priori.

The second approach is the solution of Euler equations (see for example [9]). Basically these equations describe the generation, transport and structure of the wake vorticity. The inherent dissipation of such numerical schemes causes a rapid decay of the vortical structures. Corrective measures such as higher-order numerics, finer or adaptive grids [10] add to the computational expense and still do not appear to be able to treat a full three-dimensional wake without substantial numerical diffusion.

4. Experimental Determination of Unsteady Blade Surface Pressures (and Acoustics)

Within the HELINOISE research effort [2,3,4] detailed information on both the radiated sound field and the characteristics of the unsteady surface pressures on model helicopter main rotor blades in their dependence on a wide variety of operational parameters were obtained.

4.1 HELINOISE Experimental Aspects

The experiment employed a geometrically and dynamically scaled (1:2.5) four-blade main rotor model (4 m diameter) of the BO 105 helicopter (**Fig. 1**). One of the rotor blades (NACA 23012 profile, linear twist of -8°, chord of 0.121 m) was equipped with 124 flush-mounted miniature KULITE-sensors placed at several blade sections both on the suction- and pressure-side. **Fig. 2** shows the placement of the sensors.

The model rotor setup was placed in the open-jet test section of the DNW. Simultaneously to acquiring the unsteady surface pressure data, the acoustic radiation from the rotor could be measured by means of a movable microphone array placed some distance below the rotor. The array carried 11 B&K 1/2-inch microphones, spaced at equal distances over a lateral extent of 2.7 R. It could be moved under the rotor to a (hub-relative) distance of 3 R in the upstream, 2 R in the downstream direction. The model rotor assembly itself was attached to the DNW sting support thus allowing unobstructed acoustic measurements below the rotor over a large area.

The test matrix (climb-/descent-speed vs. forward speed) for the HELINOISE project covered the entire flight operational regime of the datum helicopter with special emphasis on certain critical flight regimes such as high speed level flight and moderate speed descent, where, respectively, high speed impulsive noise and blade-vortex interaction impulsive noise occurs.

As a fully comprehensive account of the HELINOISE experiments and its results appeared in [2,3,4] only those results will be presented in the following which are pertinent to the validation efforts of the aerodynamic and acoustic codes to be discussed further down.

4.2 HELINOISE Results: Blade Pressure Data

Baseline data in terms of ensemble averaged surface pressure time histories (PTHs) for each of the 124 blade-mounted sensors were obtained simultaneously with the acoustic data for the respectively identical operational test conditions.The potential of blade surface PTHs to elucidate the physical mechanisms in the BVI noise generating process is illustrated in **Fig. 3**. Here, for a condition of moderate speed descent (δ = -6°, V = 33 m/s) such pressure time histories close to the (upper surface) blade leading edge (3% chord) at several radial stations are presented. The figure shows several vortex trails schematically superimposed on the rotating blades. From the pressure time histories one may readily discern the interactions of blade tip vortices with the rotating blade in the first and the fourth rotor quadrant.

A typical plot of upper surface pressure coefficient time histories over one rotor revolution at several chord stations x/c and 3 radial stations r/R appears in **Fig. 4**, indicating the diminishing strength of BVI down the chord.The relative strength of the interaction process at the various radial stations allows conclusions on the angle of interaction and its relative location. Such surface pressure distributions - being the basic input into the acoustic codes - need to be predicted by aerodynamic

codes with a very fine azimuthal resolution (on the order of 1°) - an immense computational effort!

The vastness of blade surface pressure time histories may be compressed for easier visual interpretation of the physical processes by plotting "isobars", i.e. lines of equal pressure (or differential pressure coefficient) for the entire rotor area instrumented, as it repeats itself for each revolution. **Fig. 5** shows such an „isobar"-plot for the same conditions as in the previous 2 figures. The traces of several vortices interacting with the blade are clearly discernible in first and fourth rotor quadrant.

4.3 HELINOISE Results: Acoustic Radiation

The initial result in measuring the radiated acoustics is a set of instantaneous or averaged pressure time histories, one for each of the microphones at any of the preselected streamwise microphone array positions. These sound pressure time histories can be readily converted into narrow band spectra, for example - such that the tonal content of the acoustic signal may be evaluated at each microphone position.

To reduce this vast amount of the ensuing individual narrow band spectra - as obtained at each test condition - is their compression into a *band pass summary level* at each microphone location. Starting from a narrow band spectrum one may add up the levels of the first few blade passage frequency (BPF) harmonics to arrive at a "low-frequency summary level, LFSL" (well suited to characterize thickness noise and the onset of high speed noise). Alternatively, one might add up the middle range of frequencies, say the levels of the 6th to the 40th rotor harmonic to arrive at a "mid-frequency summary level, MFSL" (well suited to characterize blade vortex interaction noise with its strong mid-frequency components). Such characteristic summary levels may now be plotted within the measurement area below the rotor to provide very instructive bandpass summary level contour plots.

Fig. 6 shows such a mid-frequency summary level plot under the rotor for a condition of maximum BVI-levels. Local radiation maxima occur under the advancing side (first radiation quadrant) and under the retreating side (fourth radiation quadrant). The associated PTH under the advancing side - obtained near the location of maximum levels - shows the typical intense (predominantly positive) pressure spikes. Under the retreating side - again close to the location of maximum level - the polarity of the spikes has changed into strong negative ones. The associated narrowband frequency spectra exhibit in both cases a maximum in the middle frequency range, peaking somewhere around the 10th to 15th BPF-harmonic.

If the blade surface pressure plot, shown in Fig. 5 is compared to the corresponding radiated acoustics field as shown in Fig. 6, one may readily relate the first and fourth quadrant blade vortex interaction traces on the rotor with the two strong MFSL-maxima in the first and fourth radiation quadrant under the rotor.

5. Validation of Aerodynamic Code

To demonstrate the type of prediction currently possible with advanced inviscid flow aerodynamic codes, the results of an unsteady three-dimensional panel code [11], as briefly described in Section 3, are the subject of the following considerations. The validation of the code was performed comparing the theoretical results with experimental data of the HELINOISE tests with the BO 105 model rotor as discussed in Section 4.

From the extensive test matrix of the DNW-tests, the moderate speed 6°-descent case is chosen to illustrate the code capability. A rotor in descent flight represents a fairly difficult case for the simulation but it is a very interesting situation from the acoustic point of view since during descent the wake is raised up towards the rotor disc and strong Blade/Vortex-Interaction (BVI) phenomena can occur which are responsible for intense noise generation and vibrations.

The descent flight situation computed has following parameters:

$M_{adv} = 0.740$
$C_T = 4.484 \times 10^{-3}$
$\alpha_{TPP} = 3.8°$
Advance ratio $\mu = 0.1495$

A comparison of the surface pressure distribution for the radial station r/R = 0.75 is shown in **Fig. 7** for six azimuth positions ψ = 0°, 45°, 90°, 180°, 270° and 315°. This is a representative result for other radial stations and azimuth positions.

Even though discrepancies between prediction and experiment are noticeable in the first, third and fourth quadrant, the general agreement is fair. The agreement in the leading edge region where the negative pressure peaks occur is quite good. These pressure peaks, in their time variation, contribute significantly to the sound radiation due to blade loading.

The results of Fig. 7 have been corrected for compressibility effects at each azimuth position with a simple Goethert Rule. To show the effect of a compressibility correction on the pressure distribution, the uncorrected and corrected values are plotted in Fig. 7 for the azimuth angle ψ = 270°. An improvement in the agreement with experimental data is seen mainly on the blade upper side in the vicinity of the leading edge. As a further example of the validation results, the time history of the normal force, obtained from the pressure

prediction, is compared in **Fig. 8** for the radial station r/R = 0.75 for one rotor revolution. Very good agreement is obtained between theory and experiment. The case considered is again the moderate speed 6°-descent condition. To substantiate the encouraging validation results, more test cases are in the course of being computed and will be compared with the DNW-test data.

6. Validation of Acoustic Code

In considering a complete theoretical prediction of rotor noise and observing the discrepancies between the predicted and the experimental result it is difficult to distinguish whether these might be caused by the „shortcomings" of the aerodynamic code or of the acoustic code. It is worthwhile therefore to alternatively use either reliable experimental blade pressure data or calculated blade pressure data as aerodynamic input to validate the acoustic code and to then compare the results with the experimentally determined acoustic radiation.

6.1 Acoustic Prediction using measured Blade Pressures

The DLR acoustic code AKUROT [12,13] which is based on the FWH-equation, was first validated using experimental data from an OLS-model rotor test performed in the DNW in 1982 [14]. In this code, the volume integral of the quadrupole is converted into a surface integral by applying the concept of the „momentum thickness" (first introduced by Yu, Caradonna and Schmitz [6]), thus allowing to approximately compute the quadrupole term on the basis of available blade pressure information. At that time, the predicted acoustic results had been found in good agreement with the experimental acoustic data both for BVI-cases and for high speed cases using that quadrupole approximation.

With the availability of the HELINOISE data base first AKUROT validation efforts are presently taking place, indicating very good agreement of predicted and measured acoustic radiation

6.1.1 Moderate Speed Descent Case

Fig. 9 shows for example the comparison of predicted and experimental pressure time signatures and mid-frequency summary level contour plots for the moderate speed 6°-descent „BVI-case". The agreement of the time signatures on the advancing side and on the retreating side as well as the directivity pattern in the contour plots is quite excellent. The predominantly positive acoustic pressure peaks on the advancing side can be related to the peaks in the first quadrant of the blade pressure time histories while the predominantly negative peaks on the retreating side are related to the blade pressure peaks in the 4th quadrant (see Fig. 6). Thus - as had been discussed previously - the blade pressure time signatures already allow conclusions on the radiated BVI noise.

6.1.2 High Speed Level Flight

Fig. 10 shows the comparison of experimental and calculated pressure time signatures with and without quadrupole approximation for a (moderate) highspeed case. (flight speed 80 m/s, advancing tip Mach number 0.86) at two upstream in-plane positions on the advancing and on the retreating side. It is obvious that on the advancing side the quadrupole contribution is considerable and must be accounted for while on the retreating side the quadrupole term is not as important because here the source velocity in observer direction is less compared to the advancing side.

6.2 Acoustic Prediction using calculated Aerodynamic Inputs

For a fully theoretical approach to predict the radiated rotor noise it is necessary to also predict the source aerodynamics. Several CFD codes had been applied to this end in the past to predict the rotor aerodynamics, as discussed in Section 3. For the hover case the results are generally satisfactory, but for realistic flight conditions like descent flight with BVI or highspeed conditions with highly transonic regimes near the blade tip on the advancing side the agreement with experimental blade pressures is not sufficient up to now.

6.2.1 Moderate Speed Descent Case

At DLR effort is placed on the following approaches to obtain the necessary input for the acoustic code under shock-free conditions:

- A Rotor Simulation Code - including rotor elasticity employing a lifting line method with prescribed wake model [7].

- Panel Methods such as a Lifting Body Surface Method [15] which - so far - has been successfully applied to propeller and fan noise. But for rotor noise application it works with a prescribed wake model only, up to now. Another (time efficient) Unsteady Three-dimensional Panel Method [11], which has been discussed in Section 3 above, models the interaction between the blades and their distorting free wake, eliminating the need for a prescribed wake; here the wake is part of the solution.

- A Three-dimensional EULER-Method with a prescribed wake model included [16].

Fig. 11 compares an experimentally determined mid-frequency summary level contour plot with one where calculated aerodynamic input data has been used; in this

case the input-aerodynamics (blade pressures) come from the lifting line rotor simulation code [7] .The directivity characteristics are well reproduced, but the predicted levels are too high by about 4-5 dB.

Better acoustic results are expected with aerodynamic inputs from the free wake panel method [11] as discussed in Section 3. Corresponding results are expected in the near future.

6.2.2 High Speed Level Flight

For high speed conditions only results from full-potential or Euler codes are useful because of the strong compressibility effects with the appearance of shocks on the advancing blade tip and beyond the tip.

At present at DLR an approach has been started to use results from a 3D-EULER code calculation for a high speed case [16] . In addition to the calculated blade pressures on the blade surface as input to the loading term the perturbation velocity field solution near the blade is now also inserted into the quadrupole term of the acoustic code. As described above the perturbation velocity square - the important part of the quadrupole content - is integrated at first in blade normal (or rotor plane) direction before inserting it into the acoustic code.

The method has been successfully tested for a hover case with a blade tip Mach number of 0.9. **Fig. 12** shows radiated acoustics pressure signature; here the experimental result (from the „Caradonna / Tung" experiments [17] is compared with the predicted result based on the 3D-EULER input [16] . In addition the results from a direct EULER acoustic calculation [18] is shown. The comparison indicates that with 'Euler-input' nearly the same result can be obtained as with the direct acoustic Euler calculation.

7. Conclusions

- The knowledge of the unsteady blade surface pressure distribution is crucial for assessing helicopter rotor loading noise in general and for BVI impulsive noise in particular.

- Unsteady blade pressures may be used for approximate calculation of the quadrupole term to improve thickness noise prediction at higher speed and to obtain a first order assessment of high speed impulsive noise.

- A high quality data base of unsteady blade surface pressures and the related acoustic radiation field was established by the joint European HELINOISE project, not available in Europe before.

- Prediction of unsteady blade surface pressures by high resolution aerodynamic panel methods revealed promising initial results for a typical BVI case.

- For prediction of high speed impulsive noise high resolution aerodynamic field methods are required to predict unsteady blade pressures and the perturbation velocities to enable the calculation of the quadrupole source term. This is a continuing process requiring both the improvement of the aerodynamic and acoustic codes and the development of high speed computational capabilities. At the present state only approximate solutions are feasible.

References

[1] Ffowcs Williams, J., Hawkings, D.:"Sound Generation by Turbulence and Surfaces in Arbitrary Motion", Phil.Trans.Roy.Soc. A264, 1969

[2] Splettstoesser, W. R.; Niesl, G.; Cenedese, F.; Nitti, F.; Papanikas, D.: "Experimental Results of the European HELINOISE Aeroacoustic Rotor Test in the DNW", Paper B-8, 19th European Rotorcraft Forum, Cernobbio (Como), Italy, September 1993

[3] Heller, H., Splettstoesser, W., Kloeppel, V. Cenedese, F.: "HELINOISE - The European Community Rotor Acoustics Research Program", Proceedings 15th AIAA Aeroacoustics Conference, Long Beach, USA, October 1993

[4] Splettstoesser, W. R.; Junker, B.; Schultz, K.-J.; Wagner, W.; Weitemeier, W.; Protopsaltis, A.; Fertis, D.: "HELINOISE Aeroacoustic Rotor Test in the DNW - Test Documentation and Representative Results", DLR-Mitteilung 93-09, 1993

[5] Brentner, K.S., Farassat, F.: „Helicopter Noise Prediction: The Current Status and Future Direction", DGLR/AIAA 14th Aeroacoustics Conference, Aachen, Germany, May 1992

[6] Yu, Y., Caradonna, F., Schmitz, F.: „The Influence of the Transonic Flow Field on High-Speed Helicopter Impulsive Noise"; Paper 58, 4th European Rotorcraft and Powered Lift Aircraft Forum, Italy, 1978

[7] Van der Wall, B.: „An Analytical Model of Unsteady Profile Aerodynamics and its Application to a Rotor Simulation Program", 16th European Rotorcraf tForum, Amsterdam, The Netherlands, Sep. 1989

[8] Steinhoff, J., Ramachandran, K.: „A Vortex Embedding Method for Free Wake Analysis of Helicopter Rotor Blades In Hover", AIAA Journal, Vol. 28, p. 426, 1990

[9] Kroll, N.: „Computation of the Flow Fields of Propellers and Hovering Rotors Using Euler Equations", 12th European Rotorcraft Forum, Garmisch-Partenkirchen, Germany, Paper No. 28, Sept. 1986

[10] Strawn, R. C., Barth, T. J.: „A Finite-Volume Euler Solver for Computing Rorary-Wing Aerodynamics on Unstructured Meshes", 48th AHS Forum of the American Helicopter Society, Washington, D. C., June 1992

[11] Ahmed, S., Vidjaja, V.,: "Unsteady Panel Method Calculation of Pressure Distribution on BO 105 Model Rotor Blades and Validation with DNW Test Data", to be presented at the American Helicopter Society 50th Annual Forum, Washington, DC, May 1994

[12] Schultz, K.-J., Splettstoesser, W.: "Prediction of Helicopter Impulsive Noise using Measured Blade Pressures", 43rd Annual Forum and Technology Display of the American Helicopter Society, St. Loui, MI, May 1987

[13] Schultz, K.-J., Splettstoesser, W.,: "Measured and Predicted Impulsive Noise Directivity Characteristics", 13th European Rotorcraft Forum, Arles, France, September 1987

[14] Boxwell, D. A.; Schmitz, F.H.; Splettstoesser, W. R.; Schultz, K.-J.: "Model Helicopter Rotor High-Speed Impulsive Noise: Measured Acoustics and Blade Pressures", 9th European Rotorcraft Forum, Stresa, Italy, September 1983

[15] Lohmann, D.: „Prediction of Ducted Fan Aeroacoustics with a Lifting Surface Method", DGLR/AIAA 14th Aeroacoustics Conference, Aachen, Germany, May 1992

[16] Pahlke, K., Raddatz, J.,: "3D Euler Methods for Multibladed Rotors in Hover and Forward Flight", Paper No. C20, 19th European Rotorcraft Forum, Cernobbio, Italy, September 1993

[17] Caradonna, F. X., Tung, C.: „Experimental and Analytical Studies of a Model Helicopter Rotor in Hover", NASA Technical Memorandum 81232, USAAVRADCOM TR-81-A-23, Sept. 1981

[18] Baeder, J.: „Euler Solutions to Non-linear Acoustics of Non-lifting Hovering Rotor Blades", 16th European Rotorcraft Forum, Glasgow, England, Sep. 1990

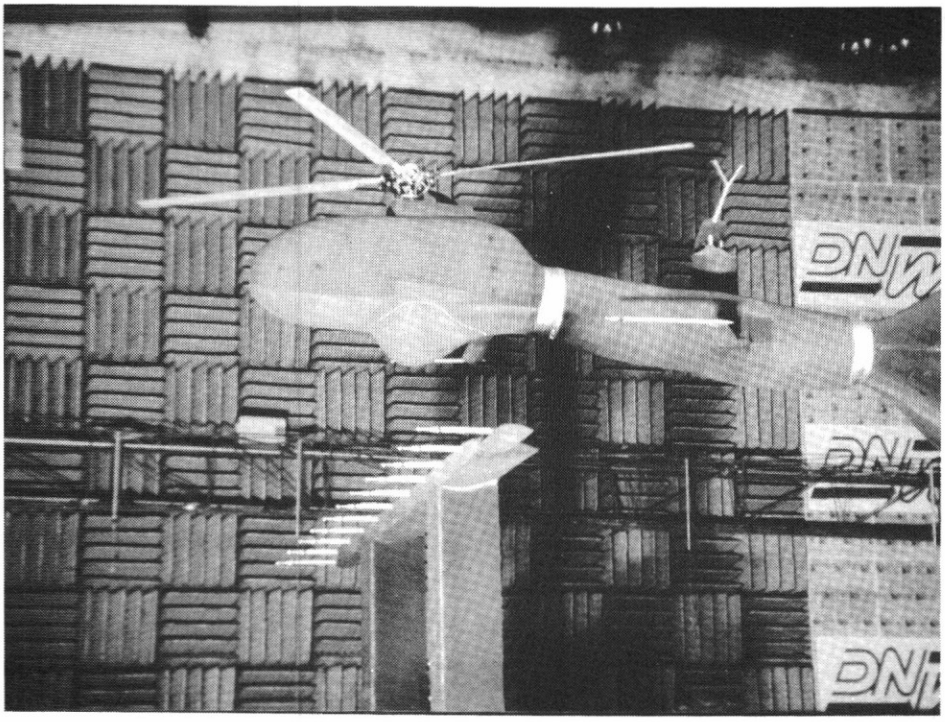

Fig. 1

HELINOISE-project test setup in the DNW for rotor aeroacouistic measurements

(gesp. Document/Heller-4)

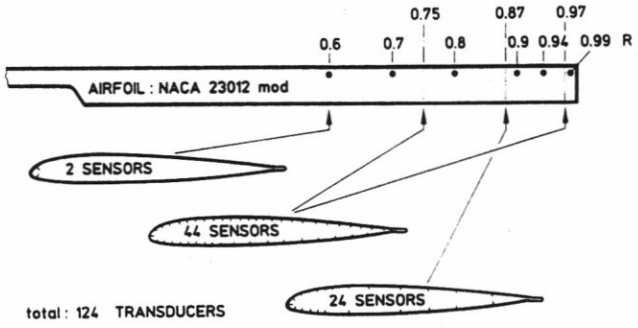

Fig. 2 Sensor placement on instrumented rotor blade

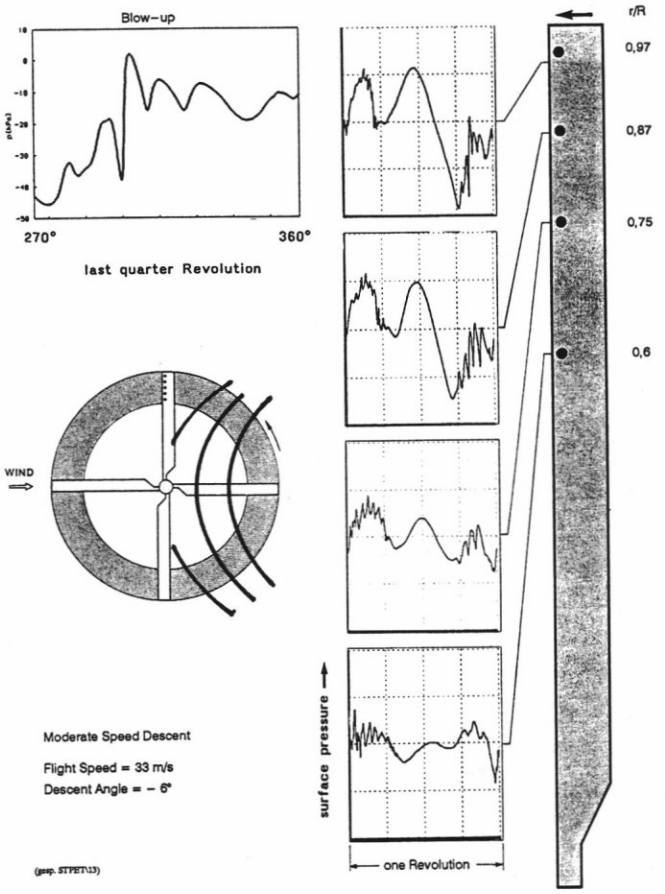

Fig. 3 Upper surface blade pressure time histories (AC part only) at several radial stations close to the leading edge for a BVI-condition of moderate speed

6°-descent:
$\mu = 0.150$;
$\alpha_{shaft} = 5.3°$;
$M_{hover} = 0.644$;
$C_T = 0.0045$

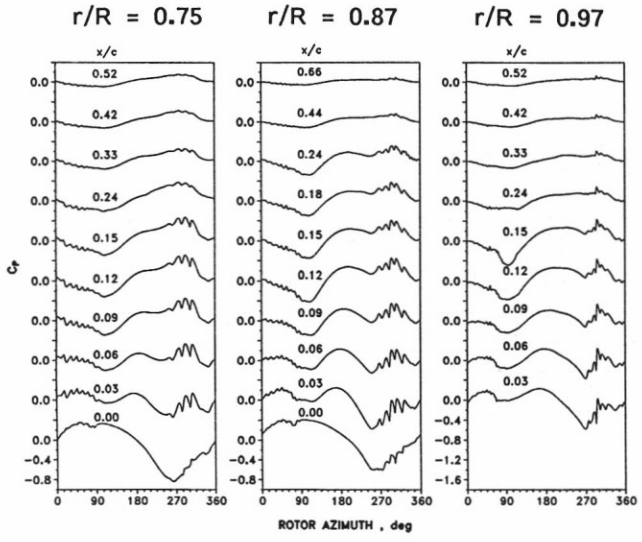

Fig. 4 Upper surface blade pressure coefficient time histories (AC part only) at different chord stations x/c for 3 radial sections r/R for conditions of moderate speed 6°-descent; other conditions as in Fig. 3

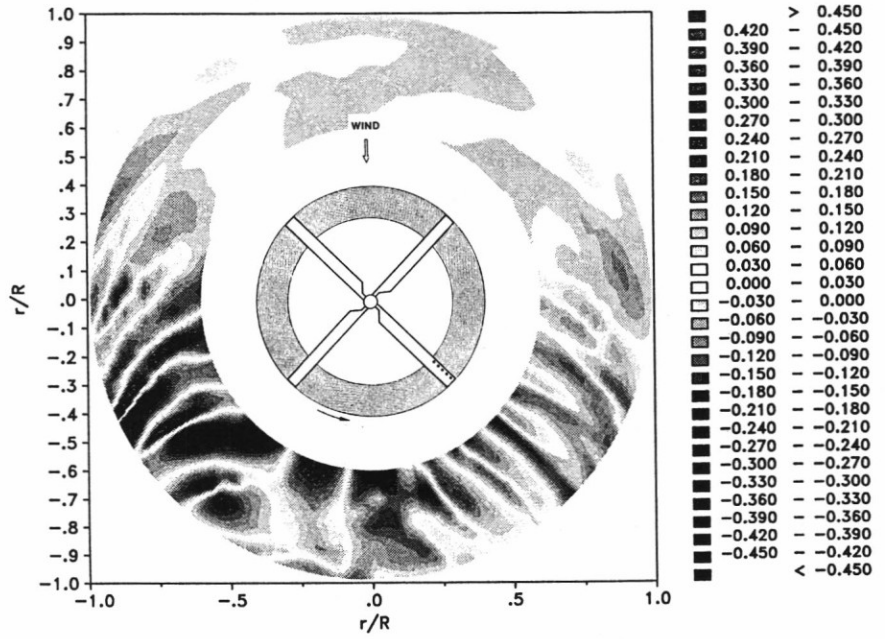

Fig. 5

Differential pressure coefficient azimu-- thal plot for one rotor revolution for sensors close to the leading edge (3% chord) and conditions of moderate speed 6°-descent; other conditions as in Fig. 3

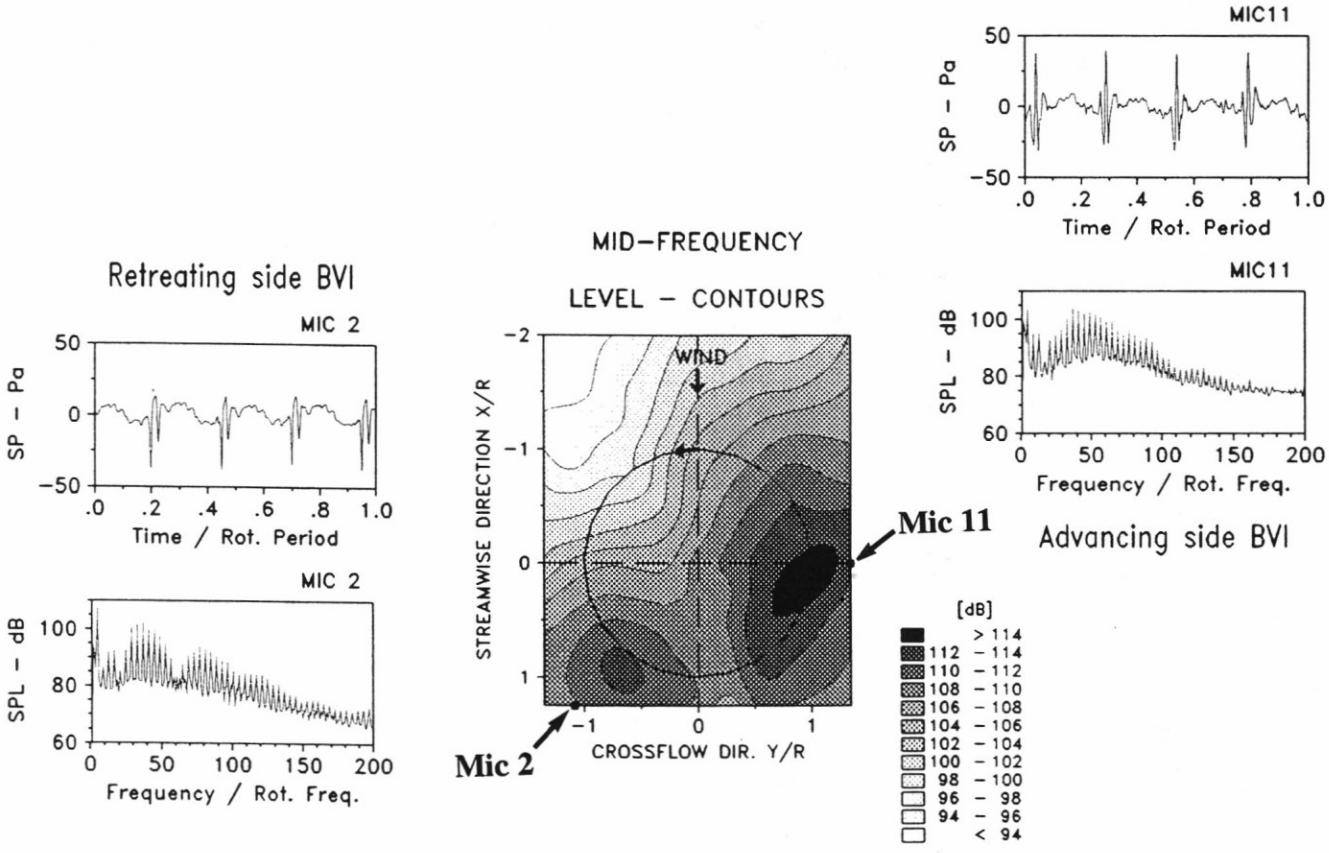

Fig. 6 Typical mid-frequency summary level contour plot and corresponding advancing side (-> Mic 11) and retreating side (-> Mic 2) BVI impulsive noise pressure time histories (upper frames) and narrowband spectra (lower frames) for conditions of a moderate speed 6°-descent; other conditions as in Fig. 3 (from Ref. 4)

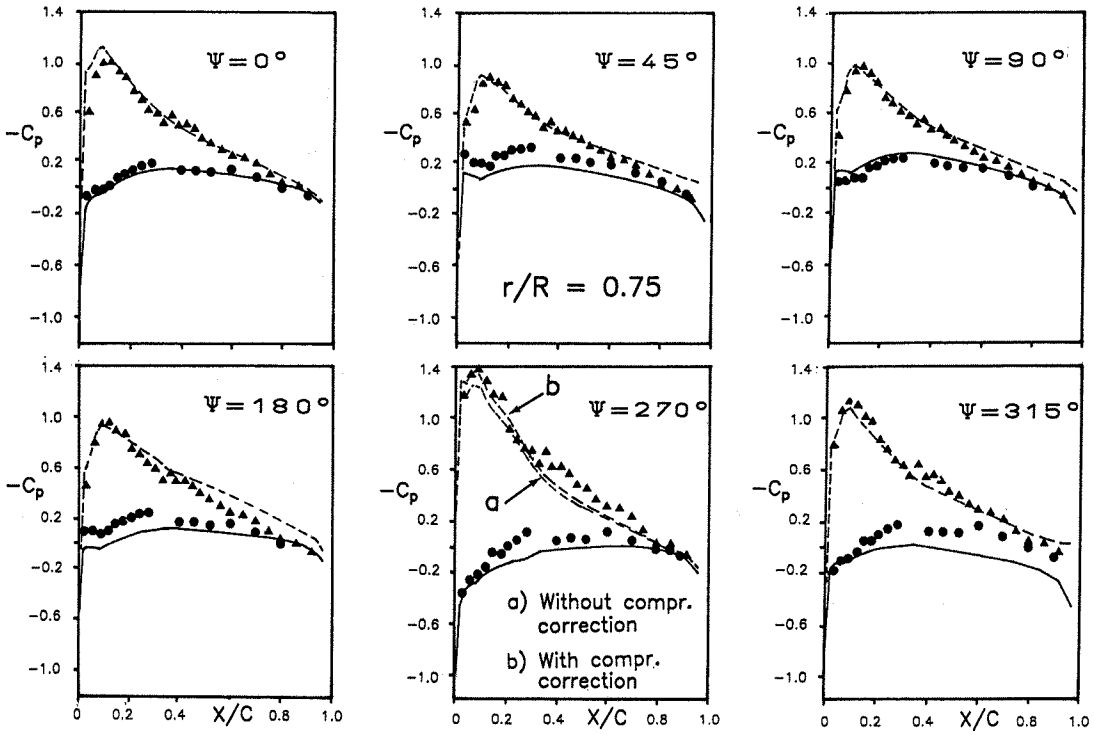

Fig. 7 Measured and predicted pressure distribution over chord at various azimuth positions for conditions of a moderate speed 6°-descent; other conditions as in Fig. 3 (from Ref. 11)

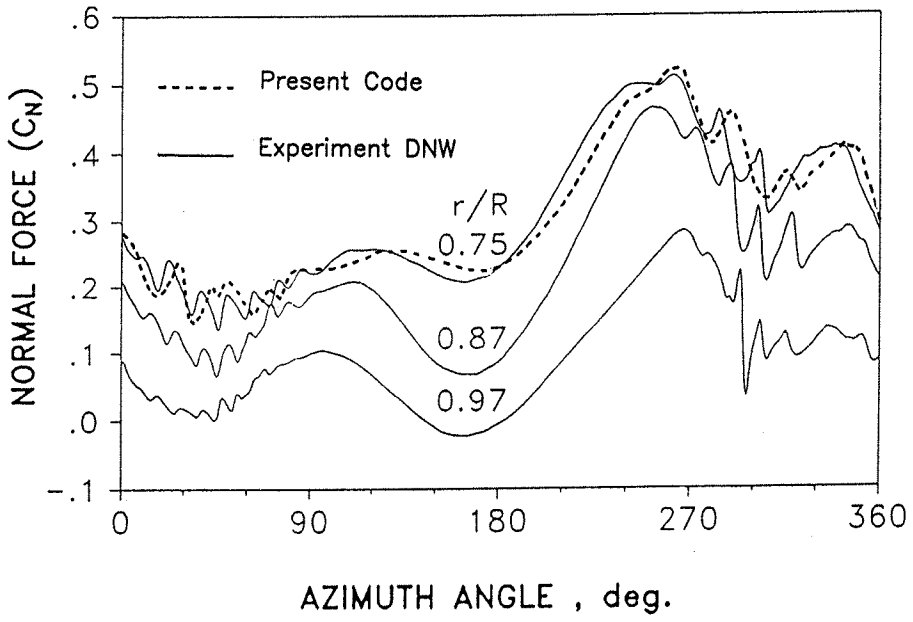

Fig. 8 Measured and predicted section normal force history over azimuth angle for conditions of a moderate speed 6°-descent; other conditions as in Fig. 3

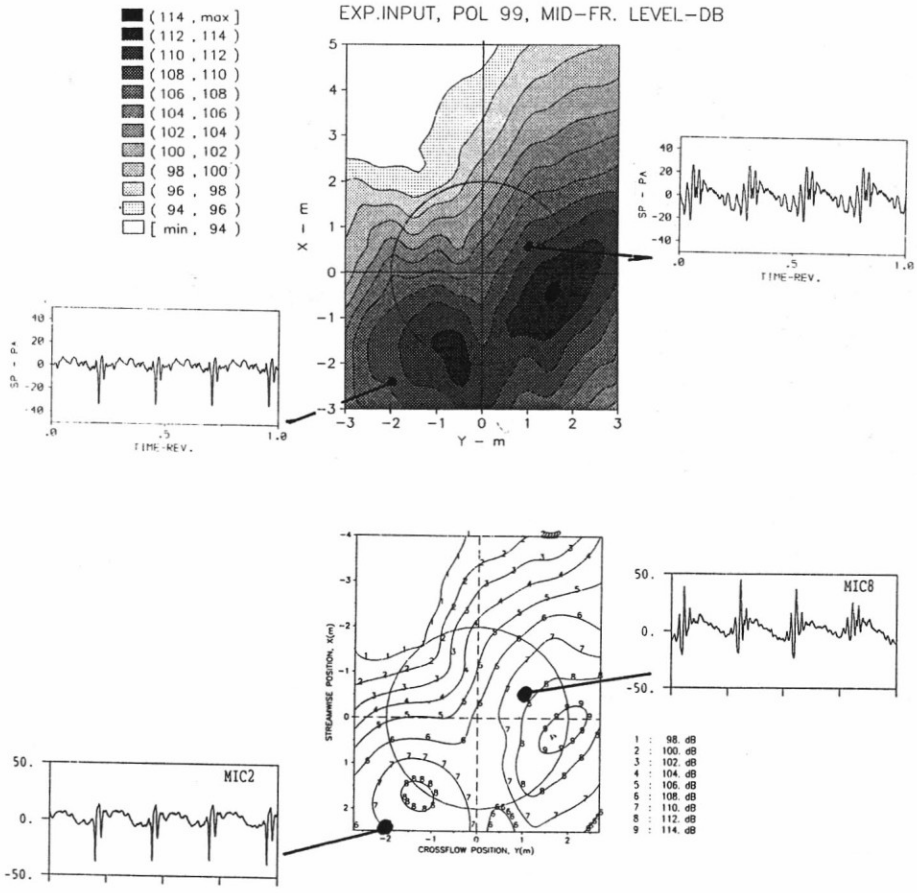

Fig. 9 Comparison of predicted and experimental time signatures and mid-frequency level contour plots for conditions of a moderate speed 6°-descent; other conditions as in Fig. 3 (prediction with experimental blade pressure input)

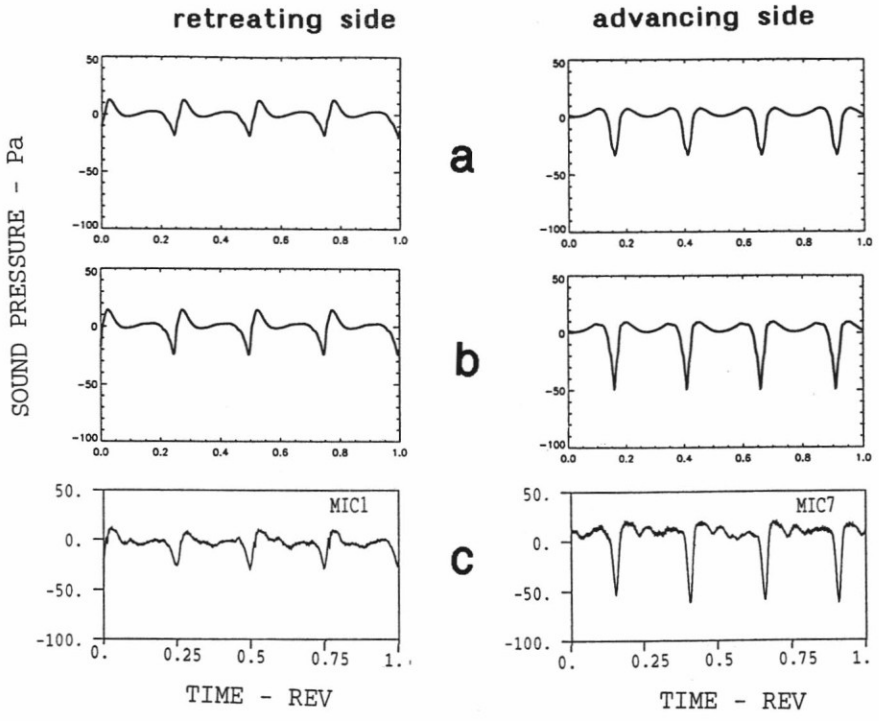

Fig. 10

Comparison of experimental and calculated acoustic pressure time signatures for a (moderate) high speed case (V = 80 m/s, M_{adv} = 0.86, experimental blade pressure input); (a) Calculation without quadrupole; (b) Calculation with approximated quadrupole; (c) Experiment; Microphone location about 0.6 rotor diameter below the rotor hub and about 1.4 rotor diameter upstream. Left column -> lateral microphone location 0.68 rotor diameter to the left (on the retreating side); right column -> lateral microphone location 0.25 rotor diameter to the right (on the advancing side)

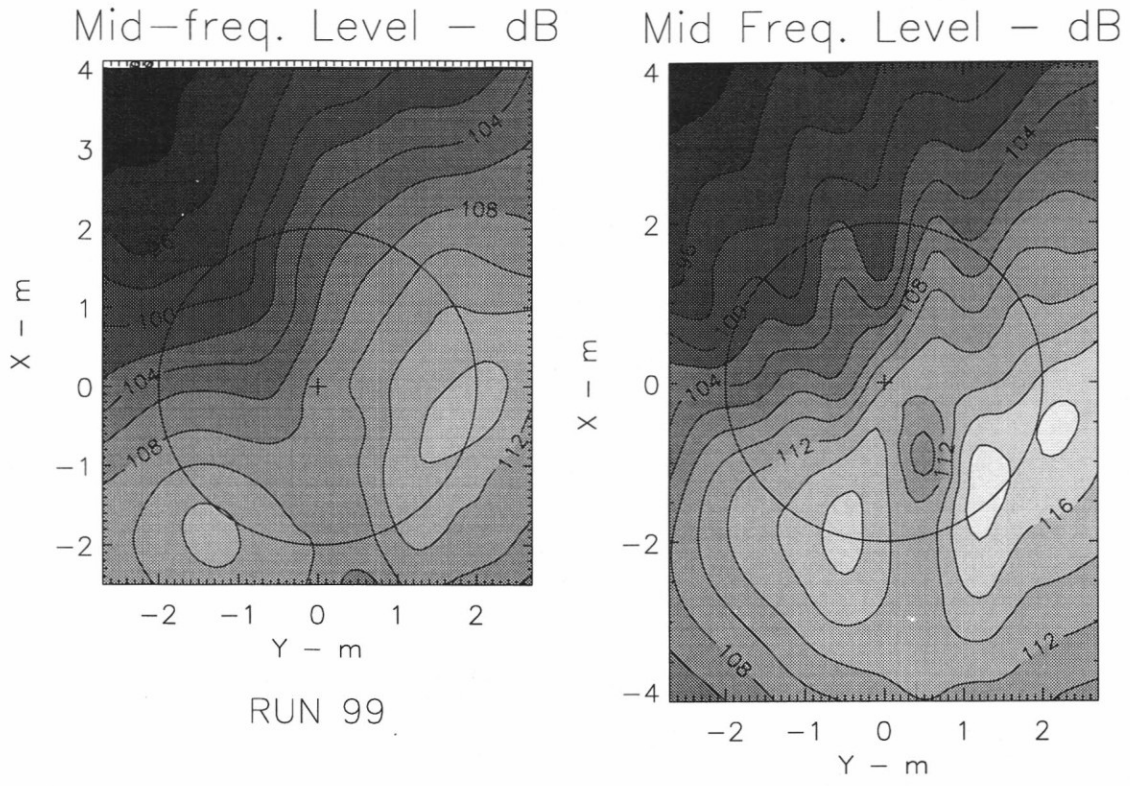

Fig. 11 Comparison of experimental (left) and calculated (right) mid-frequency level contour plots for conditions of a moderate speed 6°-descent; other conditions as in Fig. 3 (acoustic calculation with calculated loading input from lifting line rotor simulation code S4 [Ref. 7]

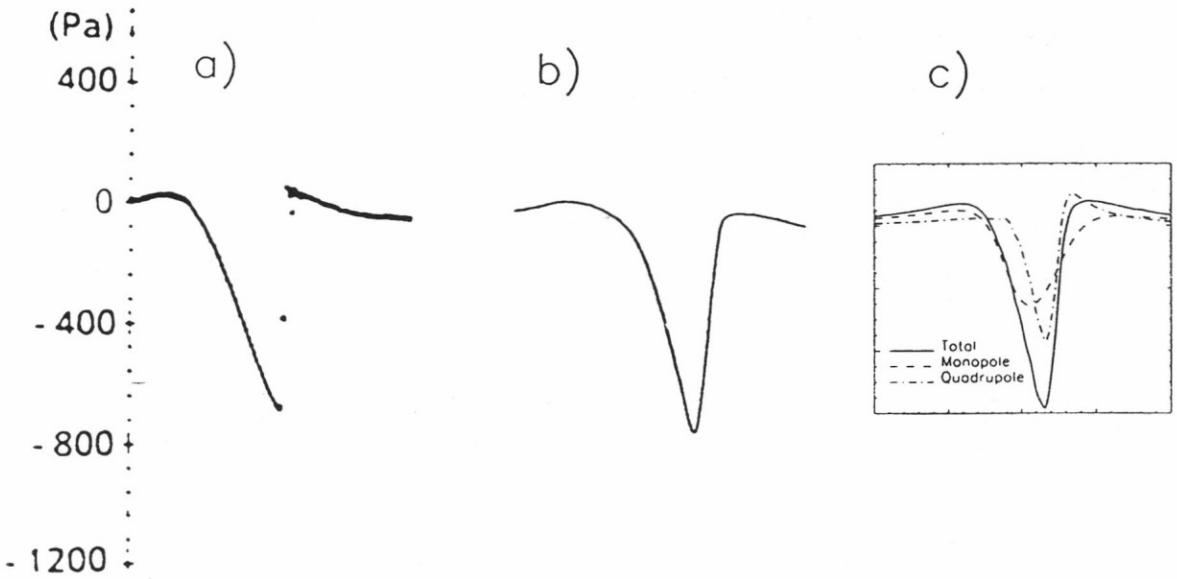

Fig. 12 Comparison of experimental and calculated acoustic pressure signatures for a high tip Mach number hover case ($M_{hover} = 0.9$); (a) Experiment (Caradonna-Tung UH 1H model rotor [Ref. 17]); (b) Direct Euler calculation [Ref. 18]; (c) Present calculation with 3D-Euler-input